Journal of Applied Physics ARTICLE scitation.org/journal/jap

Reduced strain sensitivity of the critical current of Nb_3Sn multifilamentary wires

Cite as: J. Appl. Phys. **126**, 203905 (2019); doi: 10.1063/1.5120272
Submitted: 16 July 2019 · Accepted: 11 November 2019 ·
Published Online: 26 November 2019

B. Seeber,[1,2,a)] C. Calzolaio,[3,4] D. Zurmühle,[3] V. Abächerli,[5] M. Alessandrini,[6] G. De Marzi,[7,b)] and C. Senatore[3]

AFFILIATIONS

[1]Department of Applied Physics, University of Geneva, Geneva, Switzerland
[2]scMetrology SARL, Geneva, Switzerland
[3]Department of Quantum Matter Physics, University of Geneva, Geneva, Switzerland
[4]Paul Scherrer Institut, Villingen, Switzerland
[5]Bruker EAS GmbH, Hanau, Germany
[6]Bruker Switzerland AG, Fällanden, Switzerland
[7]ENEA, Frascati, Italy

[a)]**Author to whom correspondence should be addressed:** bernd.seeber@scmetrology.ch
[b)]On leave to CERN, Geneva, Switzerland.

ABSTRACT

Strain plays an important role in Nb_3Sn multifilamentary wires because critical current depends on it and strain sensitivity of I_c increases at higher magnetic fields. In this paper, a three-dimensional strain data set becomes available by further analysis of an earlier study of the Nb_3Sn lattice parameter as a function of uniaxial applied strain at 4.2 K obtained by high-energy x-ray diffraction at the European Synchrotron Radiation Facility at Grenoble. Modeling of the angle dependence of the lattice strain with respect to the wire axis revealed that, under a specific angle, the cubic (undistorted) Nb_3Sn unit cell is independent of the applied uniaxial strain. Knowing that the critical current has its maximum for an undistorted unit cell, it is suggested to put superconducting filaments close to this specific angle with the possibility to suppress, or at least reduce, the strain sensitivity of the critical current. For this purpose, a bronze route Nb_3Sn wire was manufactured with various twist pitch lengths and with a maximum filament angle up to 38°. For the wire with the shortest twist pitch length (highest filament angle), the critical current at 19 T and 4.2 K is almost independent of the applied strain between 0.1% and 0.5%. This result confirms the theoretical/experimental considerations and opens a new way for the design and manufacture of Nb_3Sn wires and magnets.

I. INTRODUCTION

It is well known that the critical current of Nb_3Sn superconducting wires depends on uniaxial strain or stress, e.g., Refs. 1–3. In general, the critical current improves with increasing strain. After reaching a maximum, it decreases by applying further strain. An additional feature is the increasing strain sensitivity of the critical current as a function of the magnetic field. Approaching the upper critical field, it is not unusual that the critical current varies with strain in a reversible way down to almost zero.[4] The position of the maximum critical current on the strain axis, ε_m, depends on the thermally induced strain upon cooldown. In the case of the bronze route, as well as of internal tin processed Nb_3Sn wires, the matrix materials (bronze and copper) have a higher thermal expansion/contraction than Nb_3Sn filaments resulting in an axial compression on the superconductor at 4.2 K. Powder in tube (PIT) processed Nb_3Sn wires are under less thermal compression because of the presence of niobium, which has a low thermal expansion/contraction. Any axial compression reduces the critical parameters of the superconductor like T_c and B_{c2}, which also results in a smaller critical current. The behavior may be described by various empirical strain functions.[4–7] A general consideration, based on the underlying physics, came with the invariant strain function proposed by Markiewicz[8] and a further development by Bordini *et al.*[9]

The invariant strain function uses a complete set of multidimensional strains and is, therefore, the ideal tool for theoretical considerations and the analysis of experimental data. In 2012, understanding was completed by measuring the crystallographic lattice parameters of the constituents of a multifilamentary Nb_3Sn wire as a function of uniaxial strain at 4.2 K.[10] Such an investigation became possible by applying high-energy x-ray diffraction at the European Synchrotron Radiation Facility (ESRF) at Grenoble. It could be clearly shown that any change of the critical current is related to the distortion of the cubic crystallographic unit cell of Nb_3Sn and the maximum of I_c is observed for a nondistorted unit cell. Such a distortion introduces a lattice strain, which is defined by $\varepsilon(\varphi) = (a(\varphi) - a_0)/a_0$, where $\varepsilon(\varphi)$ is the lattice strain under an angle φ with respect to the wire axis, $a(\varphi)$ is the distorted lattice parameter, and a_0 is the lattice parameter of the cubic unit cell.

In this paper, data obtained in the Grenoble experiment are further analyzed by modeling the lattice strain of the Nb_3Sn unit cell as a function of angle with respect to the wire axis and of applied uniaxial strain. In Sec. II, this experiment is shortly reviewed. Section III introduces a model for the simulation of the three-dimensional lattice strain of Nb_3Sn, which is calculated as a function of applied uniaxial strain. Interestingly, it was found that under a specific angle with respect to the wire axis, the lattice strain of Nb_3Sn is zero and independent of the applied uniaxial strain. Consequently, it is postulated that the critical current must stay constant as a function of strain in the case filaments can be arranged under this specific angle. In Secs. IV and V, a Nb_3Sn multifilamentary wire with different twist pitch lengths, and therefore filament angles with respect to the wire axis, is described together with critical current measurements vs uniaxial strain. The wire with the shortest twist pitch length approaches the modeled specific filament angle, and the predicted independence of the critical current with strain is confirmed. This is followed by a discussion and conclusion in Secs. VI and VII.

II. ESRF EXPERIMENT

Detailed information of crystallographic lattice parameters of the constituents of a multifilamentary Nb_3Sn wire was obtained by high-energy x-ray diffraction at the European Synchrotron Radiation Facility (ESRF) at Grenoble.[10] The experiment was carried out at 4.2 K and as a function of uniaxial applied strain. The investigated sample volume was $0.1 \times 0.1 \times 0.81$ mm (cross section of the x-ray beam times the diameter of the wire), and the recorded x-ray diffraction pattern is an average over this volume. Sn gradients in the Nb_3Sn layer, as well as a slight ⟨110⟩ texture of Nb_3Sn in wire direction,[11] are considered but cannot be discriminated.

Two different wire layouts of an internal tin processed Nb_3Sn wire with a diameter of 0.81 mm, provided by Oxford Superconductor Technology (OST, currently Bruker OST), were investigated: a RRP™ type wire (billet number 8712) with a distributed niobium diffusion barrier and a so-called "type-I" wire manufactured for the international thermonuclear experimental reactor (ITER) toroidal field magnet (billet number 7567) with a single tantalum barrier. To approach the situation of Nb_3Sn strands in a cable-in-conduit conductor (CICC), these wires were also externally reinforced (jacketed) with a stainless steel AISI 316L tube of 0.2 mm thickness. Because qualitative results of these wires are similar, emphasis is given to the "OST type-I" wire where detailed data of critical current vs strain are available.[12]

Note that in a cable-in-conduit conductor (CICC), the differential thermal contraction between the steel jacket and the Nb_3Sn wire bundles (cable) causes a uniaxial compression of the superconductor during cooling from the temperature of the reaction heat treatment to the operating temperature. In addition, the cable is periodically bent. Moreover, during the energization of the magnet, the cable is subject to important electromagnetic forces. Another issue is the friction between individual wires (strands) of a cable. Being aware that the situation in a CICC is complex, the knowledge of the behavior of a single wire under axial compression is helpful for a further FE analysis allowing extrapolations on a larger scale, e.g. Ref. 13.

In Fig. 1, the Nb_3Sn lattice parameter at 4.2 K as a function of uniaxial strain is shown for the bare wire (a) and the stainless steel

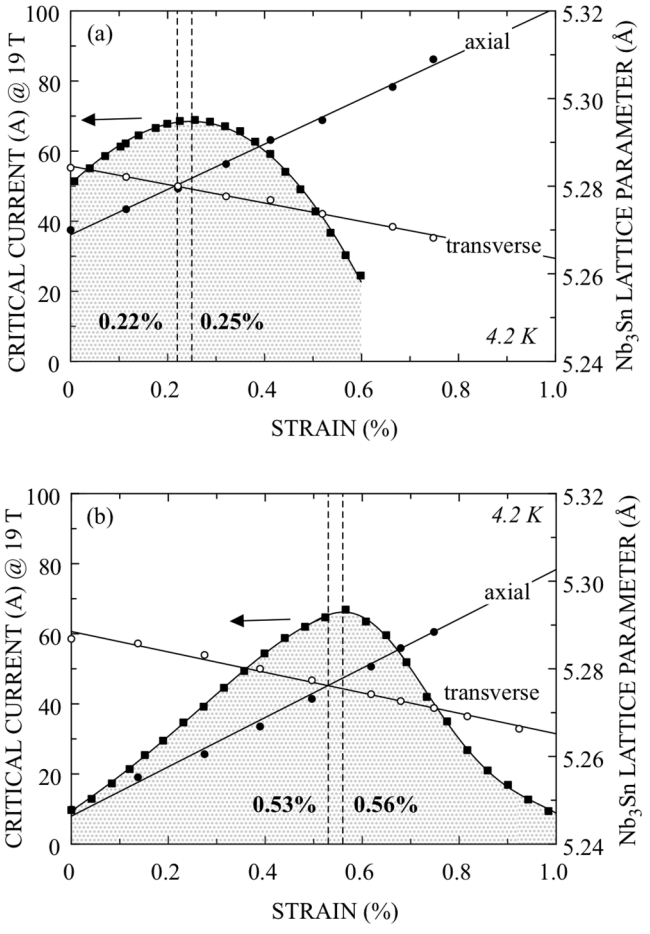

FIG. 1. Reversible critical current at 19 T and 4.2 K as a function of uniaxial strain for a bare internal tin Nb_3Sn wire (OST type-I) (a) and the same wire stainless steel reinforced (b). The crystallographic lattice parameter of Nb_3Sn in the axial and transverse direction vs strain is also shown.

jacketed one (b). In both cases, the strain window was selected to remain in the linear and elastic regime. The ESRF high-energy x-ray diffraction experiment allows us to distinguish between the axial and transverse direction with respect to the wire axis, as well as at intermediate angles. At zero applied strain, there is a distortion of the Nb_3Sn lattice cell, which is compressive in the axial and tensile in the transverse direction. In the case of the bare wire, the lattice parameter is 5.2689 Å ± 0.0006 in the axial direction and 5.2846 Å ± 0.0003 in the transverse direction. These values were obtained by a linear extrapolation of the axial and transverse lattice parameter for zero applied axial strain. With increasing applied strain, the distortion is reduced to zero at 0.22% strain, which corresponds to a cubic cell with a lattice parameter of 5.2800 Å. The critical current, I_c, was measured at 19 T and 4.2 K as a function of strain in an independent experiment.[12] Note that the variation of the critical current follows the distortion of the cubic Nb_3Sn lattice. The maximum current is observed at a strain of 0.25%. This is close to 0.22%, the value found for the cubic (not distorted) Nb_3Sn crystallographic cell. The slightly higher strain value for the maximum of I_c may be explained that filaments are not all parallel to the wire axis due to the twist pitch of about 15 mm.[12]

The situation is similar for the stainless steel jacketed wire [Fig. 1(b)]. In contrast, the distortion of the Nb_3Sn cell is much higher because of the thermal expansion/contraction of the stainless steel. Upon cooldown, stainless steel contracts substantially more than the superconducting wire, which puts the Nb_3Sn filaments under a high compressive axial load (and tensile transverse load) with an important reduction of the critical current. For comparison at zero applied strain, the axial lattice parameter of Nb_3Sn is 5.2469 Å ± 0.0007 and of the transverse one is 5.2885 Å ± 0.0005, respectively. The distortion is removed at an applied strain of 0.53% with a cubic lattice parameter of 5.2762 Å. This value is slightly smaller than that for the bare wire indicating a higher hydrostatic pressure component. Note that the shift of the maximum critical current on the strain axis with respect to the nondistorted Nb_3Sn cubic cell is the same as in the case of the bare wire.

In Fig. 2, the reversible normalized critical current at 19 T and 4.2 K vs axial lattice strain $\varepsilon = (a_{ax} - a_0)/a_0$ with a_{ax} being the lattice parameter in axial direction and a_0 being the lattice parameter of the cubic and undistorted Nb_3Sn cell is plotted for both wires (bare and reinforced by stainless steel). The maximum of I_c/I_{c0} is slightly shifted above zero axial lattice strain because all filaments are not parallel to the wire axis. The specified twist pitch length of this wire is 15 mm. Note that this shift of 0.03% is equal to that observed in Fig. 1. Without shift of the I_c/I_{c0} maximum, the axial lattice strain is identical to the commonly used intrinsic strain. The line is a polynomial fit as a guide to the eye. The dashed line presents a symmetric behavior. Note that the normalized critical current shows an asymmetry. Then, the dependence of the critical current with a positive lattice strain of Nb_3Sn is slightly increased with respect to the negative one.

III. MODELING OF THE Nb_3Sn LATTICE STRAIN

As demonstrated in Ref. 10, the lattice parameters of Nb_3Sn can be measured in any direction with respect to the wire axis

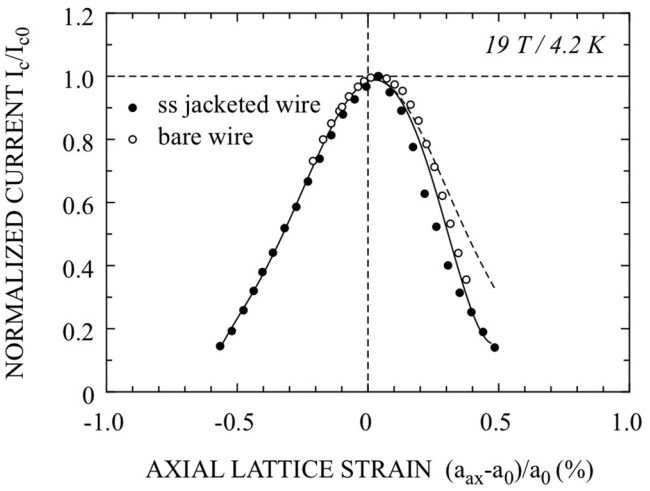

FIG. 2. Reversible normalized critical current at 19 T and 4.2 K as a function of axial lattice strain for a bare internal tin Nb_3Sn wire (OST type-I) and the same wire with stainless steel reinforcement. The maximum of I_c/I_{c0} is shifted above zero axial lattice strain because filaments are twisted. The dashed line indicates a symmetric behavior.

enabling a complete 3D data set. The analysis is time consuming and modeling is helpful. It was found that the angular dependence (with respect to the wire axis) of the Nb_3Sn lattice strain (distortion of the unit cell) can be described analytically with only two parameters, the strain in the axial and transverse direction,[10]

$$\varepsilon(\varphi) = \sqrt{(1+\varepsilon_{ax})^2\cos^2(\varphi) + (1+\varepsilon_{tr})^2\sin^2(\varphi)} - 1 \qquad (1)$$

where ε is the lattice strain, φ is the angle with respect to the wire axis, ε_{ax} is the axial lattice strain, and ε_{tr} is the transverse lattice strain. Taking the strain data from Fig. 1, the lattice strain was calculated as a function of applied axial strain, and the results are depicted in Fig. 3. Inspecting Fig. 3(a), the lattice strain is zero (no distortion of the Nb_3Sn cubic cell) and independent of the applied axial strain for an angle of 58° ± 2°. In this case, the axial strain was varied between 0% and 0.5%, which corresponds to the range of reversibility of the critical current. A similar behavior is observed for the jacketed wire with the almost same angle of 55° ± 5° [Fig. 3(b)]. Here, the axial strain was applied between 0% and 1%, which is still in the reversible regime of I_c.

Based on these results, the critical current must be independent of the applied axial strain supposing superconducting filaments can be oriented with respect to the wire axis under an angle of 58° and 55° for a bare wire and a jacketed wire, respectively. This may be achieved by an appropriate filament twist pitch length. The filament angle can be calculated as follows:

$$\tan\varphi = \frac{\pi D}{l_p}, \qquad (2)$$

where φ is the angle of a superconducting filament with respect to

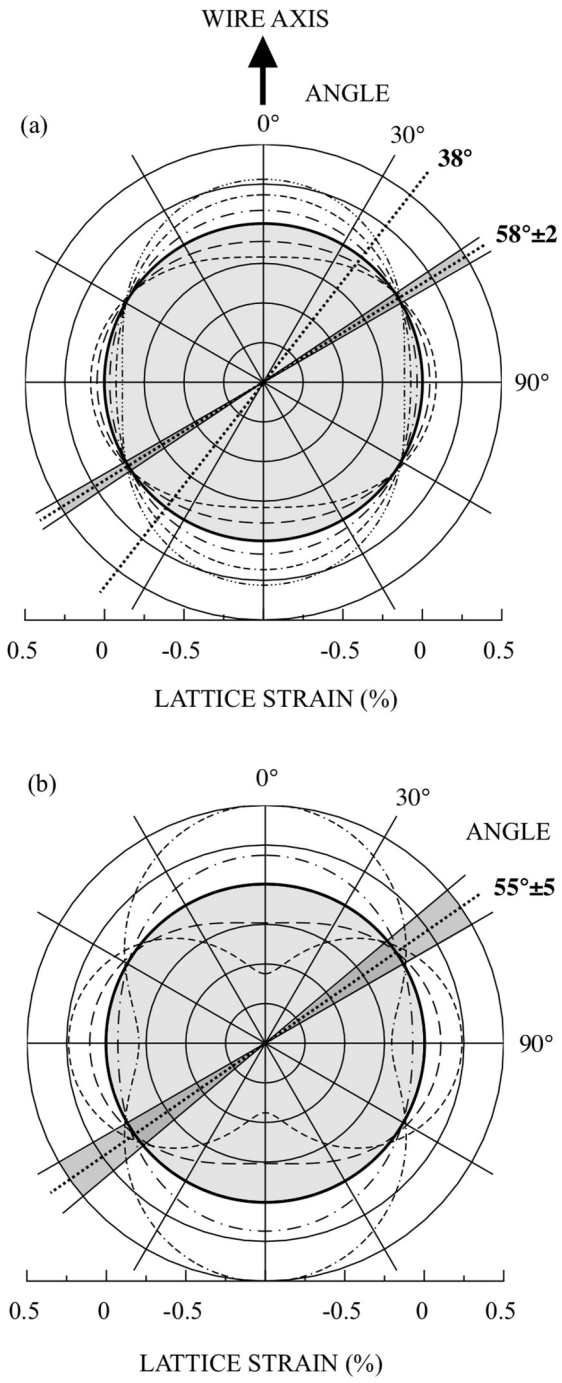

FIG. 3. Lattice strain at 4.2 K of Nb_3Sn vs angle with respect to the wire axis and applied axial strains. (a) bare wire: --- 0%, — — 0.1%, —— 0.22%, — · — 0.3%, --·-- 0.4%, and ····· 0.5%. (b) Jacketed wire: --- 0%, — — 0.3%, —— 0.53%, — · — 0.70%, and ····· 1% [See also Fig. 3(b)]. Note that the lattice strain is zero and independent of the axial strain at an angle of 58° ± 2 and 55° ± 5 for the bare wire and the jacketed one, respectively. 38° is the maximum filament angle for a twist pitch length of 5 mm and an OD of 1.45 mm.

the wire axis and positioned at a diameter D inside the wire. l_p is the twist pitch length. Taking the outer diameter (OD) of the OST type-I wire of 0.81 mm and for a filament angle of 58°, the twist pitch length must be less than 1.6 mm. No attempt was made to achieve such a twist pitch length. However, to verify the above-mentioned hypothesis, a special Nb_3Sn wire with different twist pitch lengths was manufactured by Bruker EAS.

IV. EXPERIMENTAL

A. Samples

The investigated wire is a bronze processed Nb_3Sn wire provided by Bruker EAS with an outer diameter of 1.45 mm. The diffusion barrier is niobium, and the twist pitch length varies between no twist, 50 mm, and 5 mm. An attempt to achieve a shorter twist pitch length failed. The reaction heat treatment was carried out under vacuum ($<10^{-5}$ mbar) at 570 °C/96 h and 670 °C/96 h with a heating/cooling rate of 30 °C/h. The heat treatment mandrel is oxidized stainless steel where the wire is sitting in a groove with free ends to avoid uncontrolled stress during the warm up and cooldown process. The layout of the unreacted wire is depicted in Fig. 4, and further details are given in Table I.

B. Critical current vs strain measurements

The critical current as a function of uniaxial strain was measured with a Walters spring probe (WASP).[14,15] After the reaction heat treatment on a mandrel with the same diameter (39 mm) and pitch (10 mm) as the Walters spring, the Nb_3Sn wire is transferred

FIG. 4. Micrograph of the unreacted Nb_3Sn wire provided by Bruker EAS (NSTT28105Nb23) with an OD of 1.45 mm consisting of 28 105 filaments (imbedded in a bronze matrix), a diffusion barrier of niobium, and an outer copper stabilization.

TABLE I. Selected data of the investigate bronze route Nb_3Sn wire provided by Bruker EAS.

	NSTT28105Nb23
Supplier	Bruker EAS
Wire diameter	1.45 mm
Number of subelements	511
Filament diameter	3.9 μm
Cu/non-Cu	0.30
Filament twist pitch	No twist, 50 mm, and 5 mm
Maximum filament angle	0°, 4.5°, and 38°
Barrier type	Niobium
Heat treatment	570 °C/96 h + 670 °C/96 h

to the probe and soldered only to the current terminals. This allows a strain/stress free cooldown of the sample and then the determination of the critical current at zero applied strain. If the wire sample is not strained, the critical current does not change when the Walters spring is turned in the tensile strain direction. Once strain is applied, the critical current increases. This procedure is used for a precise measurement of the zero-strain critical current. The sample length is about 1 m, corresponding to 8 turns on the WASP. Voltage taps were positioned in the central part sensing three adjacent turns each (126 mm) and one measuring the total length over almost 4 turns (484 mm). Then, the probe is warmed up to room temperature, and the sample wire is soldered over its total length on the WASP, which is required for the measurement of the irreversibility strain. Supposing that the critical current does not change with one thermal cycle, the angular position of the Walters spring for zero applied strain can be found easily. Note that a thermal cycle may reduce the contribution of the thermally induced strain of the copper stabilizer by yielding. The critical current measurement itself was carried out according to the IEC standard 61788-2. The irreversibility limit of I_c was determined by unloading the sample to ε_m, the strain for maximum critical current. As long as no filament damage occurs, the critical current after unloading increases slightly, and the irreversibility limit is determined at the strain where I_c after unloading to ε_m starts to decrease.[16]

V. RESULTS

In Fig. 5, the normalized reversible critical current vs strain at 19 T and 4.2 K is shown for the three Nb_3Sn wires with different twist pitch lengths. With respect to the untwisted wire, there is a small increase of strain sensitivity for a twist pitch length of 50 mm. The maximum critical current, averaged over three measurements (three pairs of voltage taps), is 222.6 ± 0.5 A and 218.5 ± 1.7 A for the untwisted wire and the one with a twist pitch of 50 mm, respectively. In contrast, strain sensitivity of I_c is clearly reduced in the case of the 5 mm twist pitch length, although the maximum filament angle is 38° and relatively far away from the optimal value of 58°. This unusual result was confirmed by a second measurement of another piece of wire with 5 mm twist pitch length. The only drawback is the maximum critical current is

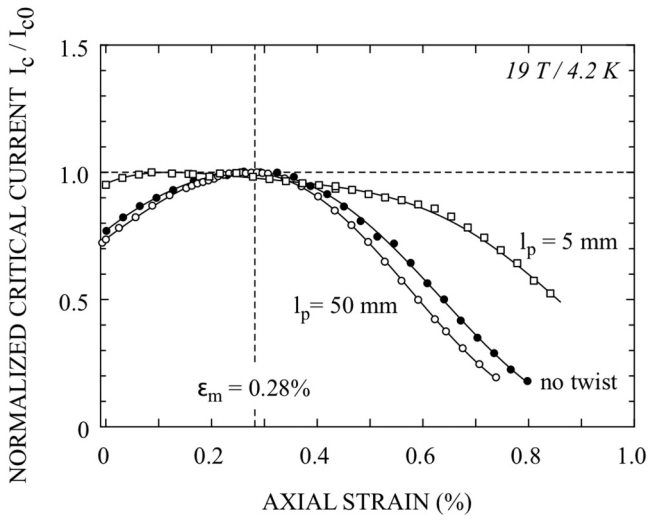

FIG. 5. Normalized reversible critical current as a function of uniaxial strain at 19 T and 4.2 K. The twist pitch length, l_p, varies between no twist, 50 mm, and 5 mm.

reduced to 86.7 A ± 0.2. The assumption that filament breakage is responsible for this reduction could not be confirmed, at least up to now (see also Sec. VI).

Figure 6 illustrates the pinning force vs field at 0.28% strain (maximum of I_c) for the wire with no filament twisting and those with 50 and 5 mm twist pitch lengths. Data are fitted using parameters of Ekin's master pinning curve for a bronze route Nb_3Sn wire.[17] At a fixed temperature, the pinning force can be written as follows:

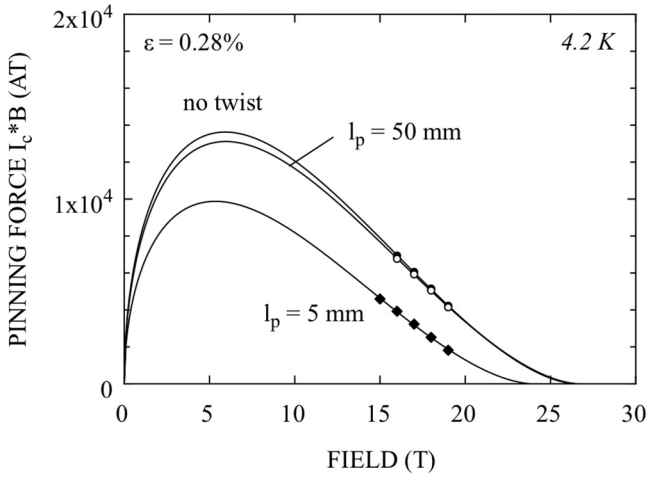

FIG. 6. Pinning force vs field at 0.28% strain (maximum of I_c) and 4.2 K for the wire without filament twist, with 50 mm, and 5 mm twist pitch length. Date are fitted with the following parameters: s = 1.2, p = 0.58, and q = 1.74.

TABLE II. Summary of B_{c2} values at 0.28% strain and at 4.2 K according to Kramer and according to Ekin together with the fitting parameter C.

Twist pitch	B_{c2}-Kramer (T)	B^*_{c2} (T)	C
No twist	27.9	26.5	875.7
50 mm	28.0	26.7	836.5
5 mm	24.9	24.0	717.1

$$F_p = I_c(B, \varepsilon)B = CB^*_{c2}(\varepsilon)^s b^p (1-b)^q, \quad (3)$$

where I_c is the critical current, B is the magnetic field, C is a fitting constant representative for the microstructure, B^*_{c2} is the effective upper critical field, and $b = B/B^*_{c2}$ is the reduced magnetic field. For a Nb_3Sn bronze route wire, the following parameters were taken: s = 1.2, p = 0.58, and q = 1.74.[17] C and B^*_{c2} are the fitting parameters that are summarized in Table II. Note that there is almost no difference in the effective upper critical field B^*_{c2} of the wire with no twist and that with a twist pitch length of 50 mm. In contrast, B^*_{c2} is reduced from 26.5 T to 24.0 T for the wire without twisting and with 5 mm twist pitch length, respectively.

VI. DISCUSSION

Inspecting Fig. 3(a), the Nb_3Sn lattice strain (distortion) is zero and independent of the axial strain at an angle of 58°. Supposing superconducting filaments can be arranged under such an angle, the critical current does not change with axial strain. In the present case, a twist pitch length of 5 mm corresponds to a maximum filament angle of 38°. In other words, filaments near the center of the wire are parallel to the wire axis and filaments close to the outer diameter are oriented under an angle of up to 38°. As can be seen in Fig. 3(a), the variation of the Nb_3Sn lattice strain as a function of uniaxial strain is reduced for filaments oriented at a higher angle. Then, part of the filaments lying at an angle of 38° enables already a reduced strain sensitivity of I_c as depicted in Fig. 5. There is a clear plateau of I_c vs strain between 0.1% and 0.5%, and the observed slope may be related to the asymmetric behavior shown in Fig. 2. In comparison, the wire with a twist pitch length of 50 mm has filament angles between 0° and 4.5°, and they are almost fully exposed to the axial strain. The higher strain sensitivity of the wire with 50 mm twist pitch with respect to the wire without filament twisting may be explained that the state of strain varies between filaments and therefore the critical current. Near the transition from the superconducting state to the normal state, in addition to the voltage generated by the flow of flux lines, a voltage appears due to current sharing between twisted filaments. It follows that the measured critical current is reduced.

Note that the original observation of lattice strain of Nb_3Sn, and the modeling, was carried out for an internal tin processed Nb_3Sn wire (OST type-I).[12] Because it was not possible to decrease the twist pitch length of this wire, a Nb_3Sn bronze processed wire with different twist pitch lengths was manufactured. It should be emphasized that the physical origin of the Nb_3Sn lattice strain does not depend on the manufacturing process.

In a more recent work, two bronze processed wires were studied by neutron diffraction at 10 K.[18] These wires were reinforced by a Cu-20 wt. %Nb matrix arranged either outside around the wire or inside. The angular dependence of the lattice strain (mentioned residual strain in the referenced paper) looks similar to Fig. 3(b) with an important axial compression of about −0.2% and −0.35% for the wire with outer and inner reinforcement, respectively. It is interesting to note that both wires show zero lattice strain at the same angle slightly above 50° with respect to the wire axis and are, therefore, supporting the observations described here.

It should be mentioned that after the reaction heat treatment, the WASP sample, which is a spiral,[15] normally keeps its diameter and pitch, but this is not the case for the wire with a 5 mm twist pitch length. After demounting from the heat treatment mandrel, for unknown reasons, the pitch was increased from 10 mm to about 18 mm. The question arises whether the original pitch of 10 mm during the reaction heat treatment is representative for zero applied strain or not. Although the question cannot be answered, the "squeezing" back from 18 mm to 10 mm, required for the critical current measurement with the Walters spring probe, was evaluated with the COMSOL Multiphysics® modeling software.[19] Reducing the pitch of the WASP sample from 18 mm to 10 mm does not introduce axial strain on the neutral axis of the wire. The situation resembles that of bending strain (tensile strain above the neutral axis and compressive strain below). The bending strain varies periodically over the length between about 0.03% and 0.06% and with a periodicity of one turn (126 mm). This observation gives confidence that such a manipulation is still in the linear regime (elastic regime) of the wire.

Finally, the reason why the critical current is substantially reduced in the wire with a twist pitch length of 5 mm is an open question and requires further investigation. A preliminary study of individual filaments over a length of about 20 mm after removal of constituents of the matrix by chemical etching did not show any difference between the Nb_3Sn wire with a 5 mm twist pitch and that without a twist pitch (no filament breakage). However, such an investigation over a short wire length is far to be representative of the total sample length of the I_c measurement (484 mm). In addition, the above-mentioned periodic bending strain of up to 0.06% cannot explain the observed behavior too.[20]

The observation that the effective upper critical field B^*_{c2} is reduced by 2.5 T with respect to the untwisted wire may explain a reduction of I_c but not completely. According to Eq. (3), the pinning force of the 5 mm twist pitch wire can be scaled back by varying B^*_{c2} from 24.0 T to 26.5 T and keeping all other parameters constant. The pinning force increases substantially but is still below that of the untwisted wire.

Another mechanism, which reduces the critical current, is the fact that filaments positioned outside of the center of the wire get longer and decrease their diameter by the twisting process. For instance, the OD of filaments close to the border of the wire goes from 3.9 μm to 2.95 μm. Then, the reduced I_c can be explained by a combination of a smaller B^*_{c2} and filament cross section. There remains the question why a short twist pitch length causes a smaller B^*_{c2}? Considering that B^*_{c2} presents an average upper critical field in a wire, a reduced B^*_{c2} means that the wire became more inhomogeneous. This is confirmed by the above-mentioned

reduction of the filament diameter and by a modified n-value, which goes from 33 to 17 at 19 T and 4.2 K for the untwisted wire and the wire with 5 mm twist pitch, respectively. Furthermore, the reaction heat treatment for a wire with a short twist pitch length is presumably no longer optimized leading to a different radial tin gradient in superconducting filaments lying in the center and close to the border of the cross section. It is known that the upper critical field of Nb_3Sn depends on the tin content (see, e.g., Ref. 21).

VII. CONCLUSION

The finding that the strain sensitivity of the critical current of Nb_3Sn multifilamentary wires may be reduced by orienting filaments at a specific angle with respect to the wire axis is obviously of practical importance. Although the ideal angle may not be achieved for all filaments, substantial improvements can already be obtained at smaller angles. For instance, inspecting Fig. 3(a) for an applied axial strain between 0% and 0.5%, filaments without twisting are exposed to a Nb_3Sn lattice strain between −0.21% and 0.28%, respectively. By contrast, for filaments lying at an angle of 38°, the Nb_3Sn lattice strain is reduced between −0.13% and 0.19%. Then, magnet designers and superconducting wire manufacturers have a tool for optimal wire or cable design. The final issue is then finding a way that electromagnetic forces acting on the superconducting wire or cable are directed outside the filament axis and that the critical current can be maintained.

ACKNOWLEDGMENTS

This work was supported in part by the Swiss National Science Foundation through the National Centre of Competence in Research, "Materials with Novel Electronic Properties, MANEP." Technical assistance from M. Wagenknecht (Bruker Switzerland AG) is thanked.

REFERENCES

[1]G. Rupp, IEEE Trans. Magn. **13**, 1565 (1977).
[2]G. Rupp, J. Appl. Phys. **48**, 3858 (1977).
[3]J. W. Ekin, IEEE Trans. Magn. **15**, 197 (1979).
[4]J. W. Ekin, Cryogenics **20**, 611 (1980).
[5]B. ten Haken, A. Godeke, and H. H. J. ten Kate, IEEE Trans. Appl. Supercond. **5**, 1909 (1995).
[6]B. ten Haken, A. Godeke, and H. H. J. ten Kate, J. Appl. Phys. **85**, 3247 (1999).
[7]D. M. J. Taylor and D. P. Hampshire, Supercond. Sci. Technol. **18**, S241 (2005).
[8]W. D. Markiewicz, Cryogenics **46**, 846 (2006).
[9]B. Bordini, P. Alknes, L. Bottura, L. Rossi, and D. Valentinis, Supercond. Sci. Technol. **26**, 075014 (2013).
[10]L. Muzzi, V. Corato, A. della Corte, G. De Marzi, T. Spina, J. Daniels, M. Di Michiel, F. Buta, G. Mondonico, B. Seeber, R. Flükiger, and C. Senatore, Supercond. Sci. Technol. **25**, 054006 (2012).
[11]M. J. R. Sandim, H. R. Z. Sandim, S. Zaefferer, D. Raabe, S. Awaji, and K. Watanabe, Scr. Mater. **62**, 59 (2010).
[12]G. Mondonico, B. Seeber, C. Senatore, R. Flükiger, V. Corato, G. De Marzi, and L. Muzzi, J. Appl. Phys. **108**, 093906 (2010).
[13]H. Bajas, D. Durville, and A. Devred, Supercond. Sci. Technol. **25**, 054019 (2012).
[14]C. R. Walters, I. M. Davidson, and G. E. Tuck, Cryogenics **26**, 406 (1986).
[15]B. Seeber, D. Uglietti, V. Abächerli, P. A. Bovier, D. Eckert, G. Kubler, P. Lezza, A. Pollini, and R. Flükiger, Rev. Sci. Instrum. **76**, 093901 (2005).
[16]B. Seeber, G. Mondonico, and C. Senatore, Supercond. Sci. Technol. **25**, 054002 (2012).
[17]J. Ekin, N. Cheggour, L. Goodrich, J. Splett, B. Bordini, and D. Richter, Supercond. Sci. Technol. **29**, 123002 (2016).
[18]S. Awaji, H. Oguro, G. Nishijima, K. Takahashi, K. Watanabe, H. Suzuki, and S. Machiya, Supercond. Sci. Technol. **23**, 105010 (2010).
[19]COMSOL Multiphysics® v. 5.4, COMSOL AB, Stockholm, Sweden, see www.comsol.com.
[20]L. Muzzi, V. Corato, R. Viola, and A. della Corte, J. Appl. Phys. **103**, 073915 (2008).
[21]Y. Li and Y. Gao, Sci. Rep. **7**, 1133 (2017).